

RESEARCH NOTES

Spectroscopic Characterization of Nickel Containing Desulfurization Sorbents

Ranjani V. Siriwardane,* Todd Gardner, James A. Poston, Jr., and Edward P. Fisher

National Energy Technology Laboratory, U.S. Department of Energy, P.O. Box 880, 3610 Collins Ferry Road, Morgantown, West Virginia 26507-0880

Angela Miltz

EG&G TSWV, Inc., 3610 Collins Ferry Road, Morgantown, West Virginia 26507

Characterization of nickel-containing desulfurization sorbents was performed by X-ray photoelectron spectroscopy, scanning electron microscopy/energy-dispersive spectroscopy, thermogravimetric analysis, and atomic absorption analysis. Sorbent pellets were tested with simulated coal-derived hot fuel gas containing H_2S , in a bench-scale fixed-bed reactor. Analysis was performed on both the interior and exterior of the sorbent pellets after both sulfidations and regenerations. In the sulfided sorbents, migration of nickel to the grain surface was observed at the exterior of the sorbent pellet. The nickel migration was less significant at the grain surface of the interior of the pellet. Changes in the oxidation state of the nickel were also observed at the outer surface of the pellet. The sulfur concentration was significantly higher at the outer surface of the pellet, indicating diffusional resistance of the fuel gas to the pellet interior.

Introduction

Removal of sulfur-containing compounds from fuel gas streams is essential for both environmental and economical concerns. Mixed metal oxide compounds containing zinc oxide as one of the components have been shown to be promising regenerable sorbents that can be utilized to remove hydrogen sulfide.¹⁻³ Nickel oxide has been utilized as one of the promoters in many of the mixed metal oxide sorbents.^{4,5} Even though nickel has been utilized in mixed metal oxide sorbents, the elemental distribution and oxidation state of nickel has not been characterized in these sorbents. Because the presence of nickel plays an important role in determining the sorbent performance, it is important to understand the changes in composition, structure, and oxidation state of nickel during reaction with hydrogen sulfide (sulfidation) and subsequent regeneration.

In this study, research was focused toward the characterization of nickel in a desulfurization sorbent after a series of reactor studies carried out in a fixed-bed flow reactor at atmospheric pressure. The characterization was performed utilizing X-ray photoelectron spectroscopy (XPS), scanning electron microscopy/energy dispersive-spectroscopy (SEM/EDS), thermogravimetric analysis (TGA), and atomic absorption analysis (AA).

Experimental Section

Sorbent pellets were prepared using 90 wt % ZnO, 5 wt % NiO, and 5 wt % bentonite. These oxides were mixed with water and the resulting paste was extruded and marumerized to obtain 3-mm-diameter spherical pellets. The pellets were calcined at 650 °C for 8 h (0 °C = 273.15 K). The sorbent pellets were tested in a fixed-bed reactor (2.54-cm bed diameter and 30.5-cm bed height). The sorbent pellets were exposed to a simulated coal-derived hot fuel gas with a composition of 1.2% (vol) hydrogen sulfide, 48.0% nitrogen, 5.5% steam, 5.4% carbon dioxide, 23.9% carbon monoxide, 1.4% methane, and 14.6% hydrogen at 538 °C and 15 psig. The sorbent was sulfided until the outlet hydrogen sulfide concentration was 500 ppmV. Regeneration of the sulfided sorbents was performed with 4% oxygen in nitrogen at 620 °C and 15 psig. The sorbent pellets were removed after each sulfidation and regeneration for analysis.

XPS spectra were obtained with a Physical Electronics Model SAM 590 equipped with a model 15-255 GAR analyzer and a 15-kV X-ray source. The instrument was calibrated using the photoemission lines, $\text{Cu}(2p_{3/2}) = 932.4 \text{ eV}$ and $\text{Au}(4f_{7/2}) = 83.8 \text{ eV}$. The binding energies were referenced to the $\text{C}(1s)$ level at 284.6 eV for adventitious carbon. All intensities reported are experimentally determined peak areas divided by the instrumental sensitivity factors. The sorbent pellets were cut in half and XPS analysis was performed on both the exterior and interior pellet surfaces. At least three sets of spectra were obtained for each sample. Intensity and binding energy values reported at a given temperature

* To whom correspondence should be addressed. Tel.: (304) 285-4513. Fax: (304) 285-4403. E-mail: ranjani.siriwardane@netl.doe.gov.

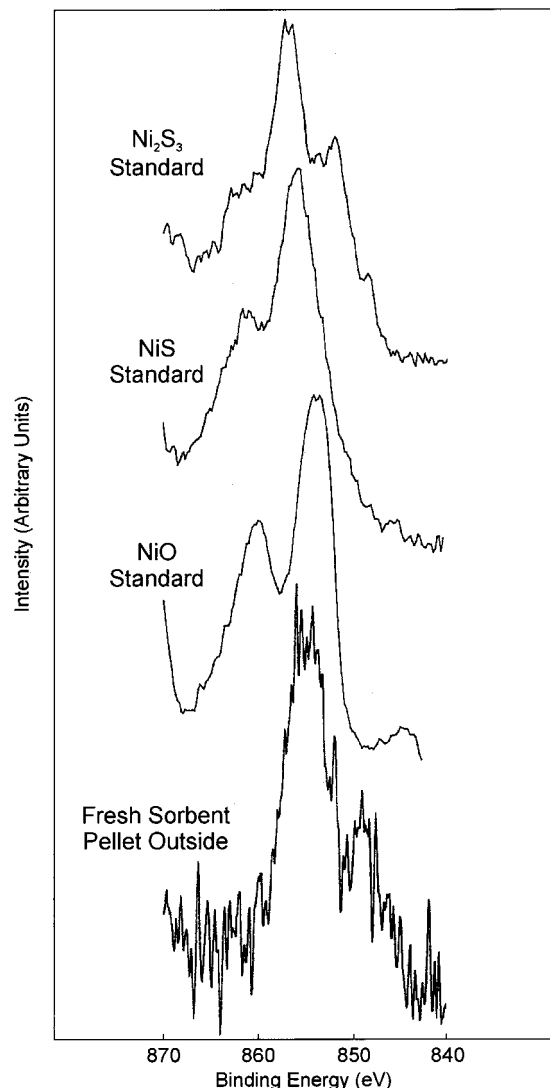


Figure 1. Ni($2p_{3/2}$) spectra of fresh sorbent pellets and standard Ni compounds.

are the average of the values obtained from the three measurements.

X-ray microanalysis was carried out using a JEOL Model 840-A scanning electron microscope which was routinely operated within a pressure range of 10^{-7} to 10^{-6} Torr (1.3×10^{-5} to 1.3×10^{-4} Pa). The JEOL-840A was interfaced to a Noran Instruments Voyager-4 X-ray microanalysis system and a Noran Instruments TN-5600 PAC system. The JEOL 840-A is equipped with a high-sensitivity, solid-state, annular backscatter electron detector, an ET-type secondary electron detector, and a Noran Instruments Micro-Z series energy-dispersive spectrometer. The spectrometer, utilizing the manganese (Alfa Puratronic) $K\alpha$ spectral line, was operated in the beryllium window mode and had a resolution of 148 eV. The microanalysis system, prior to analysis, was calibrated using a copper metal reference standard, with the centroid of the $K\alpha$ spectral peak being referenced to the energy value of 8.046 keV. X-ray microanalysis was conducted to determine both the elemental distribution and changes in elemental distribution of the sorbent pellets following sulfidation and regeneration.

TGA was conducted using a TA Instruments 951 thermogravimetric analyzer. The 951 model is a hori-

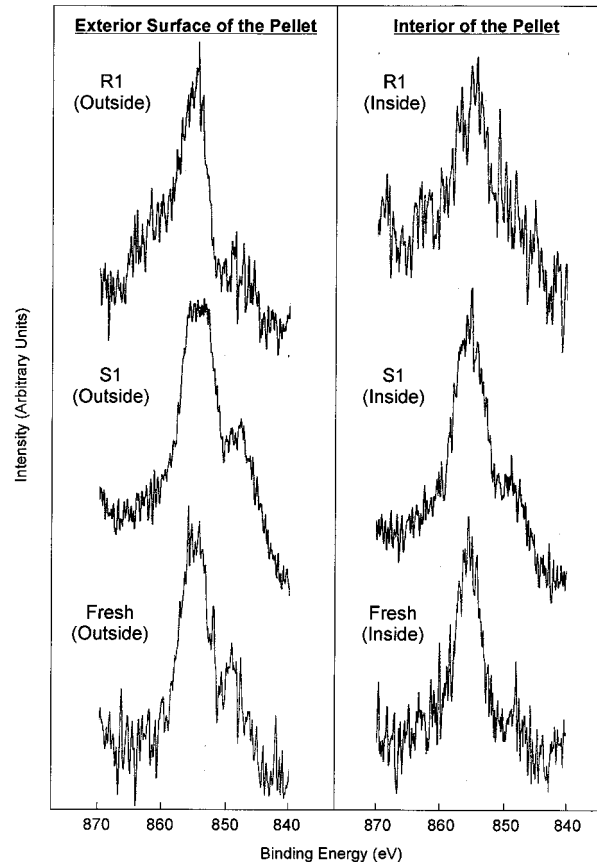


Figure 2. Ni($2p_{3/2}$) spectra of sorbent pellets after the first sulfidation and regeneration.

zontal design thermogravimetric analyzer. In the TGA experiments, pure nickel oxide was exposed to hydrogen sulfide at 538 °C and then regenerated with 6% oxygen in nitrogen at 973 °C. Samples were removed from the thermogravimetric analyzer after each sulfidation and regeneration.

Results and Discussion

XPS analysis was performed on the surface of both the exterior and the interior (cross section) of the sulfided and regenerated sorbent pellets. The Ni($2p_{3/2}$) spectra of the fresh sorbent at the outer surface are shown in Figure 1. The intensities of the nickel peaks of the fresh sorbent pellets at both the exterior and interior surface of the pellet were very low, with the spectral shapes being similar. The major Ni($2p_{3/2}$) peak was at 854.7 eV, with a very small peak also visible around 847.5 eV. The spectrum of standard nickel(II) oxide (Alfa Puratronic) is also shown in Figure 1. In addition to the major peak at 854.4 eV, a strong satellite peak around 861 eV was also present for the NiO sample. Similar satellite peaks for the nickel oxides were observed by previous researchers.⁶ The satellite peak in the nickel oxides were assigned to the $O(2p) \rightarrow Ni(3d)$ charge-transfer transition.^{6,7} These satellite peaks have not been observed in square planar nickel complexes. In the fresh sorbent pellets containing nickel, similar satellite peaks around 861 eV were not observed, as shown in Figure 1. The absence of the satellite peaks in the sorbent indicated that the nickel is not in the simple oxide form such as NiO and Ni_2O_3 .

The Ni($2p$) spectra after the first sulfidation (S1) and first regeneration (R1) are shown in Figure 2. The

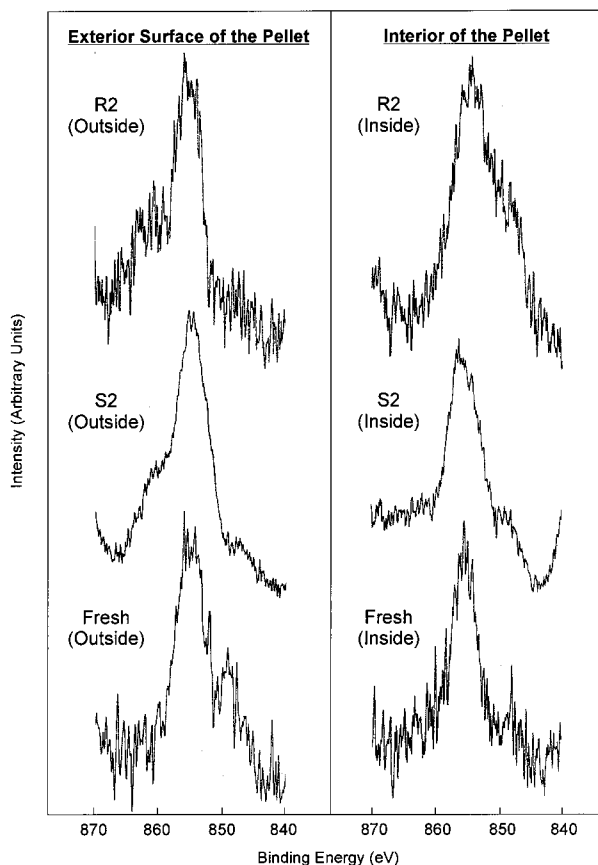


Figure 3. Ni(2p_{3/2}) spectra of sorbent pellets after the second sulfidation and regeneration.

intensity of the nickel peak at the outer surface of the pellets increased significantly after the first sulfidation. The binding energy and the general peak shape of the Ni peaks of the sulfided pellet, however, were very similar to those of the fresh sorbent. The secondary peak located at the lower binding energy (847 eV) of the main peak had a higher intensity at the outer surface of the sulfided pellet than at the interior pellet surface. The nickel spectrum of the sorbent after the first sulfidation does not appear to be similar to that of the nickel sulfides as shown in Figure 1. Thus, the nickel in the sorbent remains mostly unchanged during the first sulfidation.

Following the first regeneration, the spectrum of nickel at the outer surface was slightly different from that of the fresh sample, as shown in Figure 2. The small peak at the lower binding energy (847 eV) was not visible. However, the Ni spectrum at the interior of the pellet was similar to that of the fresh sample. Thus, this type of nickel species appears to change after the first regeneration only at the outer surface of the pellet.

The Ni(2p) spectra following the second sulfidation (S2) and regeneration (R2) are shown in Figure 3. The intensity of the Ni(2p_{3/2}) peak appeared to increase after the second sulfidation at the outer surface with the spectral structure being very similar to that after the first regeneration in which the satellite peak at 861 eV was visible. There was no change in the peak shape of the Ni(2p_{3/2}) peak at the interior of the pellet after the second sulfidation. After the second regeneration, the Ni(2p_{3/2}) peak at the outer surface had a binding energy of 856 eV with a more visible satellite peak around 861 eV, indicating some formation of nickel oxide. The higher binding energy (856 eV) of the main Ni(2p_{3/2})

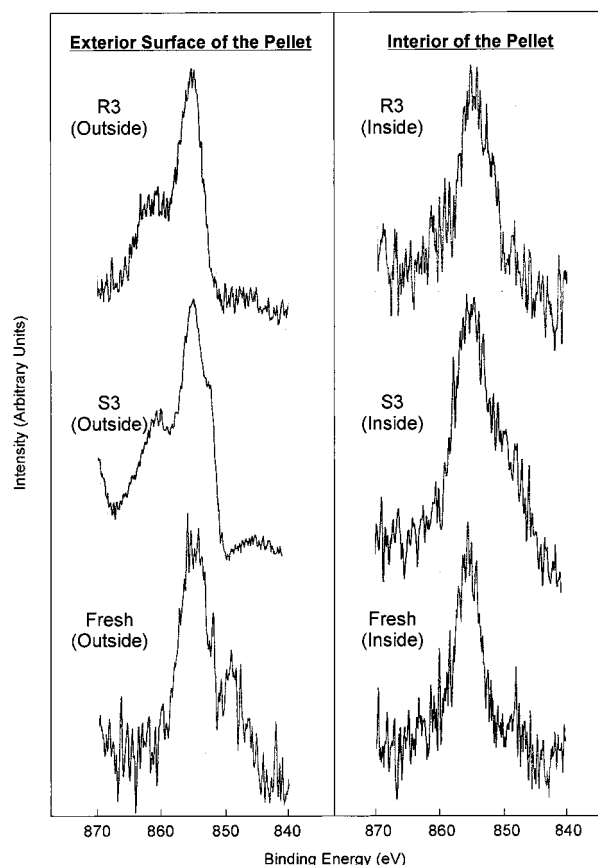


Figure 4. Ni(2p_{3/2}) spectra of sorbent pellets after the third sulfidation and regeneration.

peak may be due to the formation of Ni³⁺ species.⁶ However, at the interior of the pellet no satellite peak was visible, indicating that there was no formation of nickel oxide at the interior pellet surface.

After the third sulfidation (S3), the nickel spectrum at the outer surface was distinctly different from the previous spectra, as shown in Figure 4. In addition to the satellite peak at the higher binding energy (861 eV), a shoulder at the lower binding energy side (852.5 eV) of the main peak was observed. This spectrum was very similar to that of Ni(III) sulfide, as shown in Figure 1. Again, there were no significant changes in the nickel spectrum at the interior pellet surface. After the third regeneration (R3), the shoulder at the lower binding energy side of the main Ni peak disappeared on the outer pellet surface, as shown in Figure 4, with the spectrum appearing to be similar to that of nickel oxide, as shown in Figure 1. Thus, the type of nickel at the outer surface seems to continually change during sulfidation and regeneration, while there were no significant changes in the type of nickel on the inside pellet surface.

The Ni/Zn ratio at the outer surface of the sorbent pellets is shown in Figure 5. It is interesting to note that the Ni/Zn ratio was higher after sulfidations than regenerations. This indicates that there is a preferential migration of nickel to the outer surface during sulfidation. Following regeneration, there is again rearrangement of the nickel, with Ni/Zn ratios of the regenerated samples being very similar to those of the fresh sample. The Ni/Zn ratio after the third sulfidation is considerably higher than that at the first sulfidation. This indicated that the migration of nickel to the surface becomes progressively higher at successive sulfidations.

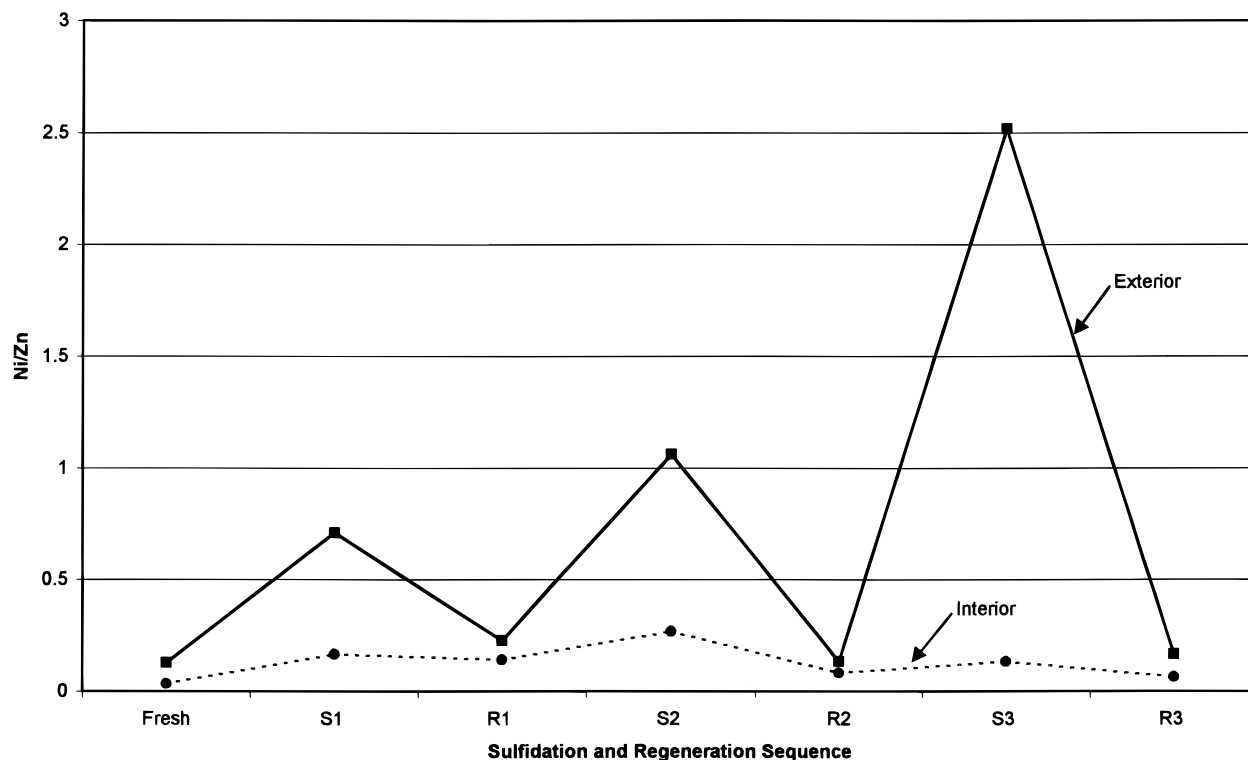


Figure 5. Ni/Zn ratio at the exterior and interior of the sorbent pellets after sulfidations and regenerations.

Similar to this observation with nickel, the migration of copper to the surface in the CuO/ZnO sorbents and migration of zinc in the zinc titanate sorbents were previously reported.^{8,9}

The Ni/Zn ratios at the grain surface of the interior pellet surface are also shown in Figure 5. The variations of Ni/Zn ratios at the grain surface of the exterior pellet surface are considerably more significant than those at the grain surface of the interior pellet surface. Even at the interior pellet surface, the Ni/Zn ratio of the sulfided samples was slightly higher than that for the regenerated samples.

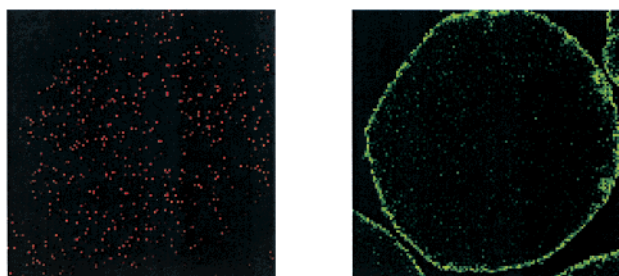
Total bulk elemental analysis conducted by atomic absorption spectroscopy indicated that there was no change in the total elemental composition after sulfidations and regeneration. This indicates that there was no loss of nickel and zinc from the pellets. Thus, the changes in the surface concentration of nickel are due to the migration of nickel within the sorbent pellet during sulfidation and regeneration. It was not possible to identify the phases of nickel with X-ray diffraction data which indicated that the nickel may be in the amorphous form.

XPS analysis was also performed on NiO powder after sulfidations and regenerations were performed in a TGA. The Ni(2p) spectra of the sulfided and regenerated samples were very similar to those of the fresh NiO sample. Sulfate formation was observed in the regenerated samples. The changes in the Ni spectra observed with the NiO powder during sulfidation and regeneration were very different from those observed in the sorbent pellets. It is possible that there is some interaction of nickel with the zinc oxide and/or bentonite (common alumina-silicate binder utilized in the preparation of sorbent pellets) in the pellets, which may have contributed to the changes in the type of nickel observed in the sorbent pellets.

X-ray microanalysis was conducted to obtain the elemental distribution of the sorbent pellets. X-ray maps

were obtained on the cross section of the sorbent pellets. Because the volume analyzed in X-ray microanalysis only contains a small portion of the top surface, the analysis obtained by this technique differs from that obtained by XPS. SEM/EDS analysis data is not necessarily representative of the sample bulk, as the penetration depth can be only a fraction of the sample depth. The penetration depth in electron microscopy is a function of several variables, among them accelerating voltage, beam current, and material composition. In these series of experiments, the depth of the X-ray interaction volume, as computed by the Kanaya-Okayana equation (10) was approximately $2.4 \mu\text{m}$. The calculations were based on an average atomic number, $n = 1.5$, and E_c equal to the characteristic energy of the K α line of the heaviest element in the compound (Zn). Calculation of the depth of the X-ray interaction volume using Proza curve software supplied with the Noran Instruments Voyager-4 microanalysis system was approximately $2.2 \mu\text{m}$.

The sulfur and nickel maps after the first sulfidation were similar to those obtained following the second sulfidation, as shown in Figure 6. As can be seen, there is a higher concentration of sulfur at the outer surface, indicating resistance to the diffusion of the fuel gas to the interior of the sorbent pellet. Nickel is uniformly distributed within the pellet and there is no increase in the concentration of nickel at the outer surface. This indicates that, macroscopically, there is no migration of nickel within the pellet during sulfidation. Thus, the nickel migration observed with XPS (approximately top 50 \AA of the surface) appears to be occurring within the individual grains. During sulfidation, the exterior surface of the pellet is exposed to the reducing gases H_2 and CO. In the presence of these reducing gases, nickel preferentially migrates to the grain surface. The sulfur layer formed outside the pellet surface makes the diffusion of these reducing gases to the interior of the pellet more restricted. Therefore, the grains inside the



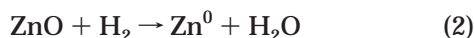
(a) Nickel Map

(b) Sulfur Map

Figure 6. Elemental maps of nickel and sulfur at the cross section of the pellet after sulfidation.

pellet did not have much exposure to the reducing gases. Hence, the nickel migration to the surface of the grains was not significant at the interior of the pellet. Similarly, the changes in the oxidation state of nickel were not significant at the interior of the pellet because the exposure to the reactive gases was limited.

Migration of nickel to the grain surface was observed only during sulfidation in the presence of reducing gases. The ability of the cations to reduce to the metallic state in the presence of reducing gases may be the driving force for the migration of these cations to the surface. Prior to the evaporation of a metal from a material, the cations have to migrate to the surface and get reduced to the metallic form at the surface. Thus, the cation with the highest reducing ability may preferentially migrate to the surface. Free energy values were calculated for the following reactions to determine the feasibility of the reduction reaction at 538 °C.



The reduction of nickel, as in reaction (1), has a free energy value of -37.1 kJ/mol while the reduction of zinc oxide as in reaction (2) has a free energy value of $+65.6$ kJ/mol. Thus, the reduction of Ni^{2+} is more favorable than the reduction of Zn^{2+} . This may be the reason for the preferential migration of nickel to the grain surface relative to zinc during exposure to the reducing gases. However, the formation of metallic nickel at the surface was not observed with XPS. The reaction of nickel with H_2S may have inhibited the formation of metallic nickel. Similarly, the reduction of copper oxide is thermodynamically more favorable than that of the zinc oxide and copper migration to the grain surface relative to zinc has been observed in the past.⁸

Summary

1. Changes in both the oxidation state and the concentration of nickel were observed at the outer surface of the sorbent pellet. Nickel migration to the grain surface at the exterior of the pellet was observed during sulfidation. Nickel concentration at the surface decreased again during regeneration.

2. Nickel was not in the simple oxide form in the fresh sorbent pellet. The changes in oxidation states of the nickel were observed at the outer surface at each sulfidation and regeneration. Nickel at the outer surface of the pellet was very similar to the Ni_2S_3 form after the third sulfidation.

3. The sulfur was mainly concentrated at the outer surface of the pellet and the diffusion of sulfur to the interior of the pellet appeared to be restricted because of the formation of the sulfur layer at the outer surface.

4. The changes in the nickel concentration at the interior of the pellet were not significant because the exposure to the reactive gases was limited as a result of the lack of diffusion.

5. Nickel migration was not observed within the sorbent pellet but the migration was observed in the individual grains at the outer surface. The migration of nickel at the exterior of the pellet may be due to the exposure of these grains to the reducing gases during sulfidation.

Acknowledgment

The authors would like to acknowledge and thank Lanny R. Golden for conducting the reactor testing. The authors would also like to acknowledge and thank the EG&G analytical staff for conducting the atomic absorption analysis.

Literature Cited

- (1) Siriwardane, R. V.; Poston, J.; Hammerbeck, K. Durable Zinc Oxide Containing Sorbents for Moving Bed and Fluid Bed Applications. Presented at the AIChE Spring National Meeting, New Orleans, LA, Symposium on High-Temperature Gas Cleaning, 1998; Paper No. 44c.
- (2) Siriwardane, R. V. *Fixed Bed Testing of Durable, Steam Tolerant Zinc Containing Sorbents*, Thirteenth Annual International Pittsburgh Coal Conference, "Coal Energy and the Environment" Proceedings 1996; Vol. 1, p 590.
- (3) Lew, S.; Jothimurugesan, K.; Flytzani-Stephanopoulos, M. High-Temperature Regenerative H_2S Removal from Fuel Gases by Regenerable Zinc Oxide-Titanium Dioxide Sorbents. *Ind. Eng. Chem. Res.* **1989**, *28*, 535.
- (4) Kidd, D. Selective Removal of Hydrogen Sulfide over Nickel Promoted Absorbing Composition. U.S. Patent, 4,990,318, 1991.
- (5) Swisher, J. H.; Schwerdtfeger, K. *Behavior of Sulfur Sorbents Containing Dispersed Nickel*, Proceedings from the 9th Annual International Pittsburgh Coal Conference; 1991; p 646.
- (6) Kim, K. S.; Davis, R. E. Electron Spectroscopy of Nickel-Oxygen. *J. Electron Spectrosc. Relat. Phenom.* **1972/1973**, *1*, 251.
- (7) Oku, M.; Hirokawa, K. The Effect of the Next Nearest Neighbor Ino on the X-ray Photoelectron Spectra of 2p Levels for Co+2, Ni+2, and Cu+2 in MgO. *J. Electron Spectrosc. Relat. Phenom.* **1977**, *10*, 103.
- (8) Siriwardane, R. V.; Poston, J. P. Characterization of Copper Oxides, Iron Oxides, and Zinc Copper Ferrite Desulfurization Sorbents by XPS and SEM. *Appl. Surf. Sci.* **1993**, *68*, 65.
- (9) Siriwardane, R. V.; Poston, J. A.; Evans, G., Jr. Spectroscopic Characterization of Molybdenum-Containing Zinc Titanate Desulfurization Sorbents. *Ind. Eng. Chem. Res.* **1994**, *33*, 2810.
- (10) Goldstein, J. I.; Newbury, D. E.; Echlin, P.; Joy, D. C.; Fiori, C.; Lifshin, E. *Scanning Electron Microscopy and X-ray Microanalysis. A Text for Biologists, Materials Scientists, and Geologists*; Plenum Press: New York, 1984; pp 73–112.

Received for review July 16, 1999

Revised manuscript received January 14, 2000

Accepted February 3, 2000